The PAMELA Space Experiment

Piergiorgio Picozza
University of Roma Tor Vergata and INFN
Via della Ricerca Scientifica 1
00133 Roma, Italy
Email: picozza@roma2.infn.it
On behalf of PAMELA Collaboration

Marco Casolino
INFN and University of Roma Tor Vergata
Via della Ricerca Scientifica 1
00133 Roma, Italy
Email: casolino@roma2.infn.it

***Abstract*— PAMELA is a satellite borne experiment designed to study with great accuracy cosmic rays of galactic, solar, and trapped nature in a wide energy range (protons: 80 MeV-700 GeV, electrons 50 MeV-400 GeV). Main objective is the study of the antimatter component: antiprotons (80 MeV-190 GeV), positrons (50 MeV-270 GeV) and search for antimatter with a precision of the order of 10^{-8}). The experiment, housed on board the Russian Resurs-DK1 satellite, was launched on June, 15^{th} 2006 in a 350×600 km orbit with an inclination of 70 degrees. The detector is constituted of a permanent magnet spectrometer core to provide rigidity and charge sign information. A Time-of-Flight system provides velocity and charge information. Lepton/hadron identification is performed by a Silicon-Tungsten calorimeter and a Neutron detector placed at the bottom of the device. An Anticounter system is used offline to reject false triggers coming from the satellite. In self-trigger mode the Calorimeter, the neutron detector and a shower tail catcher are capable of an independent measure of the lepton ($e^+ + e^-$) component up to 2 TeV. In this work we describe the experiment and its scientific objectives in the first months after launch.**

I. Introduction

The Wizard collaboration is a scientific program devoted to the study of cosmic rays through balloon and satellite-borne devices. Aims involve the precise determination of the antiproton [Boezio 1997] and positron [Boezio 2000] spectrum, search of antimatter, measurement of low energy trapped and solar cosmic rays with the NINA-1 [Bidoli 2001] and NINA-2 [Bidoli 2003] satellite experiments. Other research on board Mir and International Space Station has involved the measurement of the radiation environment, the nuclear abundances and the investigation of the Light Flash [Casolino 2003] phenomenon with the Sileye experiments [Casolino 2001], [Casolino 2005]. In this work we describe the scientific objectives, the detector and the first in-flight performance of PAMELA.

II. Scientific Goals

PAMELA aims to measure in great detail the cosmic ray component in Low Earth Orbit. Its 70^o, 350×600 km orbit makes it suited to study different items of galactic, heliospheric and trapped nature. The magnetic spectrometer and the various detectors composing PAMELA allow to study at the same time a number of different cosmic ray issues ranging over a very wide energy range, from the trapped particles in the Van Allen Belts, to electrons of Jovian origin, to the study of the antimatter component. In this section we briefly describe the main scientific objectives of the experiment, describing the detectors in the second part of the paper.

A. Antimatter research.

The study of the antiparticle component ($\overline{p}$, e^+) of cosmic rays is the main scientific goal of PAMELA. A long term and detailed study of the antiparticle spectrum over a very wide energy spectrum will allow to shed light over several questions of cosmic ray physics, from particle production and propagation in the galaxy to charge dependent modulation in the heliosphere to dark matter detection.

1) **Antiprotons:** PAMELA detectable energy spectrum of $\overline{p}$ ranges from 80 MeV to 190 GeV. Although the quality of $\overline{p}$ data has been improving in the recent years, a measurement of the energy spectrum of $\overline{p}$ will allow to greatly reduce the systematic error between the different balloon measurements, to study the phenomenon of charge dependent solar modulation, and will for the first time explore the energy range beyond $\simeq 40$ GeV. Possible excesses over the expected secondary spectrum could be attributed to neutralino annihilation; [Profumo and Ullio 2004], [Ullio 1999], [Donato 2004] show that PAMELA is capable of detecting an excess of antiprotons due to neutralino annihilation in models compatible with the WMAP measurements. Also [Lionetto 2005] estimate that PAMELA will be able to detect a supersymmetric signal in many mSUGRA models. The possibility to extract a neutralino annihilation signal from the background depends on the parameters used, the boost factor (BF) and the galactic proton spectrum. In Figure II-A.2 is shown the current status of the antiproton measurements compared with PAMELA expected measurements in three years. The curve shown refers to a secondary only hypothesis with an additional contribution of a neutralino annihilation. Also cosmological issues related to detection of a dark matter signature and search for antimatter (PAMELA will search for $\bar{H}e$ with a sensitivity of $\approx 10^-8$) will therefore be addressed with this device.

Charge dependent solar modulation, observed with the BESS balloon flights at Sun field reversal [Asaoka 2002] will be monitored during the period of recovery going from the 23^{rd} solar minimum going to the 24^{th} solar maximum. Also the existence, intensity and stability of secondary antiproton

belts [Miyasaka 2003], produced by the interaction of cosmic rays with the atmosphere will be measured.

2) **Positrons:** A precise measurement of the positron energy spectrum is needed to distinguish dark matter annihilation from other galactic sources such as hadronic production in giant molecular clouds, e^+/e^- production in nearby pulsars or decay from radioactive nuclei produced in supernova explosions. PAMELA is capable to detect e^+ in the energy range 50 MeV to 270 GeV. In Figure II-A.2 is shown the current status of the positron measurements compared with PAMELA expected measurements in three years, with the additional contribution coming from neutralino annihilation. Possibilities for dark matter detection in the positron channel depend strongly on the nature of dark matter, its annihilation cross section and the local inhomogeneity of the distribution. [Hooper and Silk 2004] performed different estimation of PAMELA sensitivity according to different hypothesis of the dark matter component: detection is possible in case of an higgsino of mass up to 220 GeV (with BF=1) and to 380 GeV (with BF=5). Kaluza Klein models [Hooper and Kribs 2004] would give a positron flux above secondary production increasing above 20 GeV and thus clearly compatible with PAMELA observational parameters. In case of a bino-like particle, as supposed by Minimal Supersymmetric Standard Model, PAMELA is sensible to cross sections of the order of $2 - 3 \times 10^{-26}$ (again, depending of BF). In case of Kaluza Klein excitations of the Standard Model the sensitivity of PAMELA is for particles up to 350 and 550 GeV. In the hypothesis of the littlest Higgs model with T parity, the dark matter candidate is a heavy photon which annihilates mainly into weak gauge bosons in turn producing positrons. In [Asano 2006] is shown that PAMELA will be able to identify this signal if the mass of the particle is below 120 GeV and the BF is 5. In [Hisano 2006] is assumed a heavy wino-like dark matter component, detectable with PAMELA in the positron spectrum (and with much more difficulty in the antiproton channel) for mass of the wino above 300 GeV. This model predicts that if the neutralino has a mass of 2 TeV the positron flux increases by several orders of magnitude due to resonance of the annihilation cross section in W^+W^- and ZZ: in this scenario not only such a signal would be visible by PAMELA but also be consistent with the increase of positrons measured by HEAT [Barwick 1999]. In conclusion a detailed measurement of the positron spectrum, its spectral features and its dependence from solar modulation will either provide evidence for a dark matter signature or strongly constrain and discard many existing models.

B. Galactic Cosmic Rays

Proton and electron spectra will be measured in detail with PAMELA. Also light nuclei (up to O) are detectable with the scintillator system. In this way it is possible to study with high statistics the secondary/primary cosmic ray nuclear and isotopic abundances such as B/C, Be/C, Li/C and $^3He/^4He$. These measurements will constrain existing production and propagation models in the galaxy, providing detailed information on the galactic structure and the various mechanisms involved.

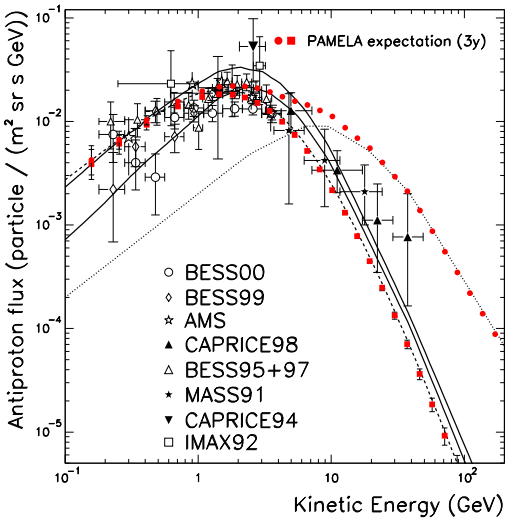

Fig. 1. Recent experimental $\overline{p}$ spectra (BESS00 and BESS99 [Asaoka 2002], AMS [Aguilar 2002], CAPRICE98 [Boezio 2001-a], BESS95+97 [Orito 2000], MASS91 [Hof 1996], CAPRICE94 [Boezio 1997], IMAX92 [Mitchell 1996]) along with theoretical calculations for pure $\overline{p}$secondary production (solid lines: [Simon 1998], dashed line: [Bergstrom 1999]) and for pure $\overline{p}$ primary production (dotted line: [Ullio 1999], assuming the annihilation of neutralinos of mass 964 GeV/c^2)

C. Solar modulation of GCR

Launch of PAMELA occurred in the recovery phase of solar minimum toward cycle solar maximum of cycle 24. In this period it will be possible to observe solar modulation of galactic cosmic rays due to increasing solar activity. A long term measurement of the proton, electron and nuclear flux at 1 AU will provide information on propagation phenomena occurring in the heliosphere. As already mentioned, the possibility to identify the antiparticle spectra will allow to study also charge dependent solar modulation effects.

D. Solar energetic particles

We expect about 10 significant solar events during the experiment's lifetime with energy high enough to be detectable [Shea 2001]. The observation of solar energetic particle (SEP) events with a magnetic spectrometer will allow several aspects of solar and heliospheric cosmic ray physics to be addressed for the first time.

1) Protons: PAMELA will be able to measure the spectrum of cosmic-ray protons from 80 MeV up to almost 1 TeV and therefore will be able to measure the solar component over a very wide energy range (where the upper limit will be limited by statistics). These measurements will be correlated with other instruments placed in different points of the Earth's magnetosphere to give information on the acceleration and propagation mechanisms of SEP events. Up to now there has been no direct measurement [Miroshnichenko 2004] of the

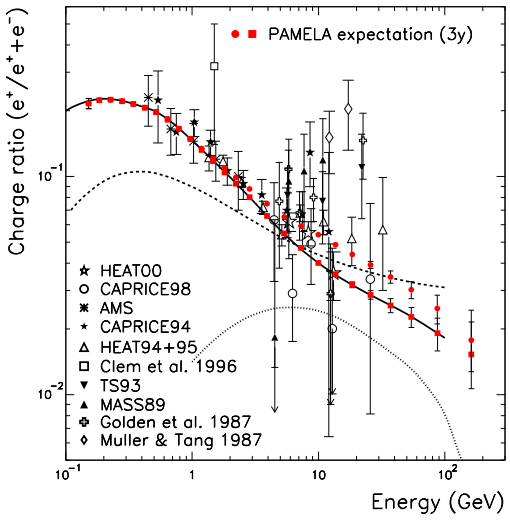

Fig. 2. The positron fraction as a function of energy measured by several experiments ([Golden 1987], [Muller 1987], [Clem 1996] and MASS89 [Golden 1994], TS93 [Golden 1996], HEAT94+95 [Barwick 1998], CAPRICE94 [Boezio 2000], AMS [Alcaraz 2000], CAPRICE98 [Boezio 2001-b], HEAT00 [Beatty 2004]). The dashed [Protheroe 1982] and the solid [Moskalenko 1998] lines are calculations of the secondary positron fraction. The dotted line is a possible contribution from annihilation of neutralinos of mass 336 GeV/c^2 [Baltz 1999]. The expected PAMELA performance, in case of a pure secondary component (full boxes) and of an additional primary component (full circles), are indicated in both panels. Only statistical errors are included in the expected PAMELA data.

high energy (>1 GeV) proton component of SEPs. The importance of a direct measurement of this spectrum is related to the fact [Ryan 2000] that there are many solar events where the energy of protons is above the highest (≃100 MeV) detectable energy range of current experiments, but is below the detection threshold of ground Neutron Monitors [Bazilevskaya 1998]. However, over the PAMELA energy range, it will be possible to examine the turnover of the spectrum, where we find the limit of acceleration processes at the Sun. Over 80 MeV we expect about 2×10^6 particles/day (assuming a spectral index of γ = 3 we have 2×10^3 events / day above 1 GeV).

2) Electrons and Positrons: Positrons are produced mainly in the decay of π^+ coming from nuclear reactions occurring at the flare site. Up to now, they have only been measured indirectly by remote sensing of the gamma ray annihilation line at 511 keV. Using the magnetic spectrometer of PAMELA it will be possible to separately analyze the high energy tail of the electron and positron spectra at 1 Astronomical Unit (AU) obtaining information both on particle production and charge dependent propagation in the heliosphere in perturbed conditions of Solar Particle Events.

3) Nuclei: PAMELA can identify light nuclei up to Carbon and isotopes of Hydrogen and Helium. Thus we can investigate into the light nuclear component related to SEP events over a wide energy range. This should contribute to establish whether there are differences in the composition of the high energy (1 GeV) ions to the low energy component (≃ 20 MeV) producing γ rays in the quiescent solar corona[Ryan 2005]. Applying the same estimates as above, we can expect ≃10^4 ^{4}He and ≃10^2 ^{3}He nuclei for gradual events, and more for impulsive (often ^3He enriched) ones. Such a high statistics will allow us to examine in detail the amount of the ^{3}He and deuterium (up to 3 GeV/c). These measurements will help us to better understand the selective acceleration processes in the higher energy impulsive [Reames 1999] events.

4) Neutrons: Neutrons are produced in nuclear reactions at the flare site and can reach the Earth before decaying [Chupp 1982]. The neutron detector will measure in great detail the temporal profile and distribution of solar neutrons. On the occurrence of solar events, neutrons are expected to reach Earth before protons as they have no charge. They are not deflected by any magnetic field and will be directly recorded by PAMELA (if it is not in Earth's shadow).

5) Lowering of the geomagnetic cutoff: The high inclination of the orbit of the Resurs-DK1 satellite will allow PAMELA to study [Ogliore 2001], [Leske 2001] the variations of cosmic ray geomagnetic cutoff due to the interaction of the SEP events with the geomagnetic field.

E. Trapped particles

The 70^o orbit of the Resurs-DK1 satellite allows for continuous monitoring of the electron and proton belts. The high energy ($> 80MeV$ component of the proton belt, crossed in the South Atlantic region will be monitored in detail with the magnetic spectrometer. Using the scintillator counting rates it will be possible to extend measurements of the particle spectra to lower energies (3.5 MeV for e^- and 36 MeV for p). In this way it will be possible to perform a detailed mapping of the Van Allen Belts showing spectral and geometrical features. Also the neutron component will be measured, although some care needs to be taken to estimate the background coming from proton interaction with the main body of the satellite.

F. Jovian Electrons

Since the discovery made by the Pioneer 10 satellite of Jovian electrons at about 1 AU from Jupiter [Simpson 1974], [Eraker 1982], with an energy between 1 and 25 MeV, several interplanetary missions have measured this component of cosmic rays. Currently we know that Jupiter is the strongest electron source at low energies (below 25 MeV) in the heliosphere within a radius of 11 AUs. Its spectrum has a power law with spectral index γ = 1.65, increasing above 25 MeV, where the galactic component becomes dominant. At 1 AU from the Sun the IMP-8 satellite could detect Jovian electrons in the range between 0.6 and 16 MeV and measure their modulation by the passage of Coronal Interaction Regions (CIR) with 27 days periodicity [Eraker 1982], [Chenette 1980]. There are also long term modulation effects related to the Earth-Jupiter synodic year of 13 months duration. In fact, since Jovian electrons follow the interplanetary magnetic field lines, when the two planets are on the same solar wind spiral line, the electron transit from Jupiter to the Earth is eased and the flux increases.

On the other side, when the two planets lie on different spiral lines the electron flux decreases. For PAMELA the minimum threshold energy for electron detection is 50 MeV. In this energy range, however, geomagnetic shielding will reduce the active observation time reducing total counts. Nevertheless it will be possible to study for the first time the high energy Jovian electron component and test the hypothesis of reacceleration at the solar wind Termination Shock (TS). It is known that cosmic rays originating outside the heliosphere can be accelerated at the solar wind TS. This applies also to Jovian electrons, which are transported outward by the solar wind, reach the TS and undergo shock acceleration thus increasing their energy. Some of these electrons are scattered back in the heliosphere. The position of the shock (still unknown and placed at about 80–100 AU) can affect the reaccelerated electron spectrum [Potgieter 2002], [Fichtner 2001]. Overall, Jovian electrons are dominant in the energy range 50-70 MeV and decrease in intensity to about 1% of the total galactic flux in the above 70 MeV. This component can however be extracted from the galactic background with observation periods of the order of four-five months [Casolino 2004]. In addition it is possible that the reacceleration of electrons at the solar wind TS is modulated by the solar cycle; three years of observations in the recovering phase of the solar minimum should show such effects.

G. High energy lepton component

The calorimeter can provide an independent trigger (with geometrical factor of 400 $cm^2\ sr$ to PAMELA for high energy releases due to showers occurring in it. In this way it is possible to study the global electron and positron flux in the energy range between 300 GeV and 2 TeV, where measurements are currently scarce [Kobayashi 1999]. At this energy discrimination with hadrons is performed with topological and energetic discrimination of the shower development in the calorimeter coupled with neutron information coming from the neutron detector. This is because neutron production cross-section in an e.m. cascade is lower than in a hadronic cascade[Galper 2001].

III. Instrument Description

In this section we describe the main characteristics of PAMELA detector; a more detailed description of the device and the data handling can be found in [Picozza 2006], [Casolino 2004-a], [Casolino 2004-b]. The device (Figure 4) is constituted by a number of highly redundant detectors capable of identifying particles providing charge, mass, rigidity and beta over a very wide energy range. The instrument is built around a permanent magnet with a silicon microstrip tracker with a scintillator system to provide trigger, charge and time of flight information. A silicon-tungsten calorimeter to perform hadron/lepton separation. A shower tail catcher and a neutron detector at the bottom of the apparatus increase this separation. An anticounter system is used to reject spurious events in the off-line phase. Around the detectors are housed the readout electronics, the interfaces with the CPU and all

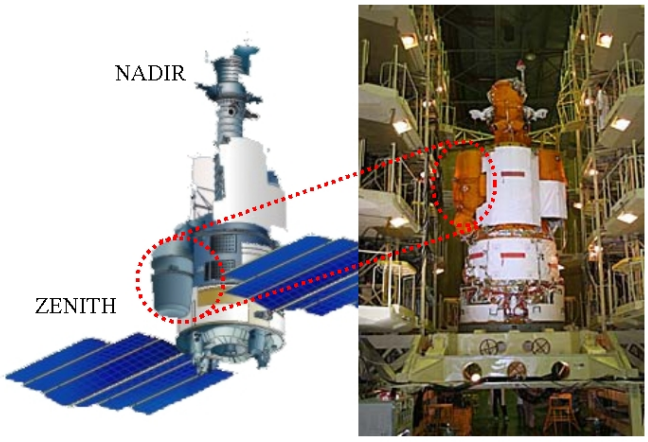

Fig. 3. Left: Scheme of the Resurs-DK1 satellite. PAMELA is located in the pressurized container on the left of the picture. In the right panel is shown a picture of the satellite in the assembly facility in Samara. The dashed circle between the shows the location of PAMELA pressurized container.

primary and secondary power supplies. All systems (power supply, readout boards etc.) are redundant with the exeption of the CPU which is more tolerant to failures. The system is enclosed in a pressurized container (Figure 3,5) located on one side of the Resurs-DK satellite. In a twin pressurized container is housed the Arina experiment, devoted to the study of the low energy trapped electron and proton component. Total weight of PAMELA is 470 kg; power consumption is 355 W, geometrical factor is $21.5 cm^2 sr$.

A. Magnetic Spectrometer

The permanent magnet [Adriani 2003] is composed of 5 blocks, each divided in 12 segments of Nd-Fe-B alloy with a residual magnetization of 1.3 T arranged to provide an almost uniform magnetic field along the y direction. The size of the cavity is $13.1 \times 16.1 \times 44.5\, cm^3$, with a mean magnetic field of 0.43 T. Six layers of $300 \mu\, m$ thick double-sided microstrip silicon detectors are used to measure particle deflection with $3.0 \pm 0.1\ \mu m$ and $11.5 \pm 0.6\ \mu m$ precision in the bending and non-bending views. Each layer is made by three ladders, each composed by two $5.33 \times 7.00\, cm^2$ sensors coupled to a VA1 front-end hybrid circuit. Maximum Detectable Rigidity (MDR) was measured on CERN proton beam to be $\simeq 1\, TV$.

B. Scintillator / Time of Flight

The scintillator system[Barbarino 2003] provides trigger for the particles and time of flight information. There are three scintillators layers (S1, S2, S3), each composed by two orthogonal planes divided in various bars. S1 and S3 bars are 7 mm thick and S2 bars are 5 mm. TOF determination is 250 ps for protons and 70 ps for C nuclei (determined with beam tests in GSI), allowing separation of electrons from antiprotons up to $\simeq 1$ GeV and albedo rejection. The scintillator system is also capable of providing charge information up to $Z = 8$.

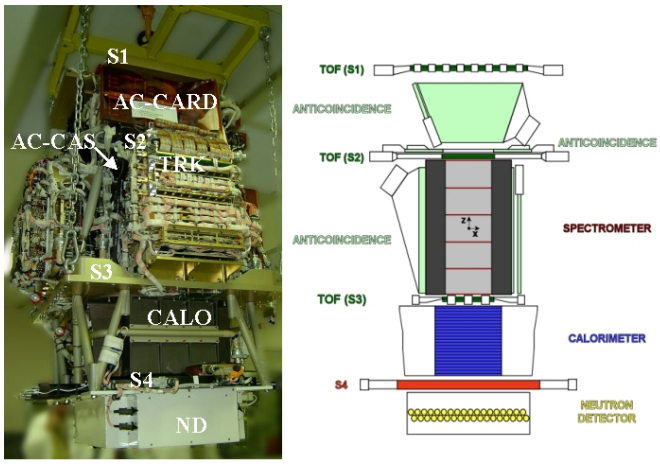

Fig. 4. Left: Photo of the PAMELA detector during the final integration phase in Tor Vergata clean room facilities, Rome. It is possible to discern, from top to bottom, the topmost scintillator system, S1, the electronic crates around the magnet spectrometer, the baseplate (to which PAMELA is suspended by chains), the black structure housing the Si-W calorimeter, S4 tail scintillator and the neutron detector. Right: scheme - approximately to scale with the picture - of the detectors composing PAMELA.

Fig. 5. Photo of Resurs in the final integration phase in Baikonur. PAMELAis being integrated in the right pressurized container.

C. Silicon Tungsten Calorimeter

Lepton/Hadron discrimination is performed by the Silicon Tungsten sampling calorimeter [Boezio 2002] located on the bottom of PAMELA . It is composed of 44 silicon layers interleaved by 22 0.26 cm thick Tungsten plates. Each silicon layer is composed arranging 3×3 wafers, each of $80 \times 80 \times .380\, mm^3$ and segmented in 32 strips, for a total of 96 strips/plane. 22 planes are used for the X view and 22 for the Y view in order to provide topological and energetic information of the shower development in the calorimeter. Tungsten was chosen in order to maximize electromagnetic radiation lengths (16.3 X_o) minimizing hadronic interaction length (0.6 λ). The CR1.4P ASIC chip is used for front end electronics, providing a dynamic range of 1400 mips (minimum ionizing particles) and allowing nuclear identification up to Iron. The calorimeter can also function in self trigger mode requiring the release of energy above 150 mip in all the 24 views of planes from 7 to 18. As mentioned, in this way the geometrical factor of the calorimeter is 400 $cm^2 sr$ (rejecting events coming from the satellite, which are recognized by the shower development).

D. Shower tail scintillator

This scintillator ($1cm \times 48 \times 48\, cm^3$) is located below the calorimeter and is used to improve hadron/lepton discrimination by measuring the energy not contained in the shower of the calorimeter. It can also function as a standalone trigger for the neutron detector.

E. Neutron Detector

The $60 \times 55 \times 15\ cm^3$ neutron detector is composed by 36 ^3He tubes arranged in two layers and surrounded by polyethylene shielding and a 'U' shaped cadmium layer to remove thermal neutrons not coming from the calorimeter. It is used to improve lepton/hadron identification by detecting the number of neutrons produced in the hadronic and electromagnetic cascades. Since the former have a much higher neutron cross section than the latter, where neutron production comes essentially through nuclear photofission, it is estimated that PAMELA overall identification capability is improved by a factor 10. As already mentioned, the neutron detector is used to measure neutron field in Low Earth Orbit and in case of solar particle events as well as in the the high energy lepton measurement.

F. Anticoincidence System

To reject spurious triggers due to interaction with the main body of the satellite, PAMELA is shielded by a number of scintillators used with anticoincidence functions[Orsi 2004], [Pearce 2003]. CARD anticoincidence system is composed of four 8 mm thick scintillators located in the area between S1 and S2. CAT scintillator is placed on top of the magnet: it is composed by a single piece with a central hole where the magnet cavity is located and read out by 8 phototubes. Four scintillators, arranged on the sides of the magnet, make the CAS lateral anticoincidence system.

IV. Integration and Launch

Pamela was integrated in INFN - Rome Tor Vergata clean room facilities, Rome; tests involved first each subsystem separately and subsequently the whole apparatus simulating all interactions with the satellite using an Electronic Ground Support Equipment. Final tests involved cosmic ray acquisitions with muons for a total of about 480 hours. The device was then shipped to TsKB Progress plant, in Samara (Russia), for installation in a pressurized container on board the Resurs-DK satellite for final tests. Also in this case acquisitions with cosmic muons (140 hours) have been performed and have

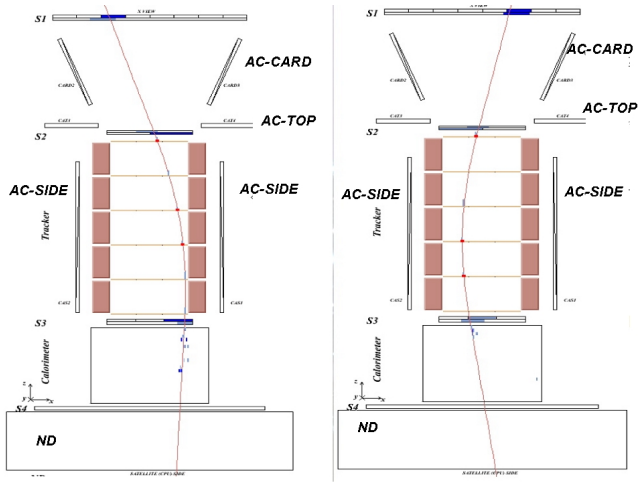

Fig. 6. Left: A positron event of 0.171 GeV detected with PAMELA. The particle crosses the top Scintillators (S1 and S2), the magnet spectrometer, the Bottom scintillator (S3) and is stopped in the Silicon Calorimeter. Right: An electron event of 0.169 GeV. In both cases only the projection on the bending view is shown. Note the opposite curvature which allows to identify sign of the charge of the particles.

shown the correct functioning of the apparatus, which was then integrated with the pressurized container and the satellite. In 2006 the final integration phase took place in Baikonur cosmodrome in Kazakstan.

Launch occurred with Soyuz-U rocket on June 15^{th} 2006, 08:00:00.193 UTC, orbital insertion was in a parking orbit of semimajor axis of 6642 km. Final boost occurred on June 18^{th} 2006 when the orbit was raised to a semimajor axis of 6828 km.

Altitude of the satellite is usually minimum in the northern hemisphere and maximum in the southern hemisphere since its primary goal is to perform earth observations and resolution of the pictures increases at lower altitudes. To compensate for atmospheric drag, the altitude of the satellite is periodically reboosted by vernier engines. To perform this manoeuvre the pressurized container housing PAMELA is folded back in the launch position, the satellite is rotated 180^o on its longitudinal axis and then engines are started. Reboost frequency depends from orbital decay, due to atmospheric drag, in turn caused by solar activity. Up to October 2006 the activity has been low with only two small Solar Particle Events, so there has not been the need to perform this maneuver yet. Resurs-DK1 oscillates on its longitudinal axis when performing Earth observations: a detailed information of the attitude of the satellite is provided to the CPU of PAMELA in order to know the orientation of the detector with precision of $\simeq 1$ degree.

V. In flight data

PAMELA was first switched on June, 26^{th} 2006. Two events acquired with PAMELA are shown in Figure 6. It is possible to see the particles crossing the scintillators and the magnet and being stopped in the calorimeter. Due to the opposite charge the particles are bent in opposite direction by the magnetic field. A typical behaviour of the acquisition of

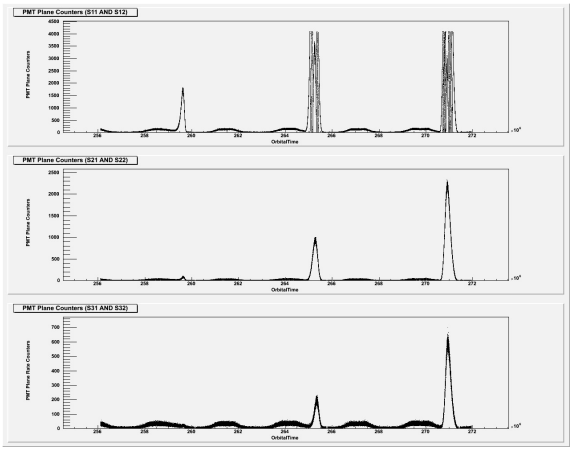

Fig. 7. Counting rates of PAMELA (ADC channels) as a function of time (ms).

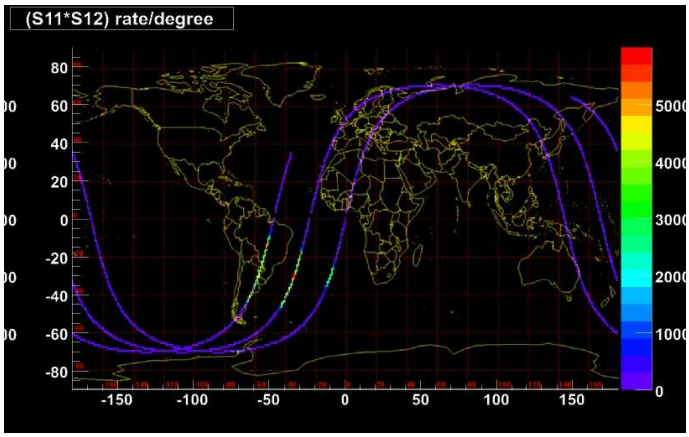

Fig. 8. Ground track of PAMELA with counting rate of S11*S12 trigger. Note the particle rate increase in the South Atlantic Anomaly

the device is shown in Figure 7. The three panels show the counting rate of the three planes and correspond to particles of increasing energy: S11*S12 is triggered by 36 MeV protons and 2.5 MeV e^-, S21*S22 requires protons and electrons of 9.5 and 63 MeV respectively and S31*S32 requires protons and electrons of 80 MeV and 50 MeV (lower energy particles may penetrate the detector from the sides and increase the trigger rate). The higher energy cut is evident in the counting rate of the scintillators: the first SAA passage, corresponding to the easternmost passage is absent in the S3 counting rate. The other two passages in the SAA saturate several times the ADC counting rate of the S1 scintillator but not the other two scintillators. This is consistent with due to the power law spectrum of trapped particles in the SAA and the geometrical ratio between the two scintillators. Also S2 and S3 counting rate ratio in the anomaly is about 5, consistent with a particle flux ratio evaluated with AP8 algorithm [Gaffey and Bilitza 1994]. Outside the SAA it is possible to see the increase of particle rate at the geomagnetic poles due to the lower geomagnetic cutoff. The highest rates are found when the satellite crosses

the trapped components of the Van Allen Belts. In Figure 8 it is possible to see the same trigger rate as a function of the ground track of PAMELA. It is possible to see the inclination of the orbit of satellite and the particle rate increase in the polar and South Atlantic regions. The pause in the acquisition at the equator are due to the calibration of the subdetectors usually performed during the ascending phase to avoid crossing the radiation belts. In Figure 9 is shown PAMELA world particle rate for S1*S2 counter, exibiting the high latitude electron radiation belts and the proton belt in the South Atlantic Anomaly. Note that the northern electron belt is less intense than the southern one because PAMELA orbit is $\simeq 350$ km in that region as compared to the $\simeq 600$ km in the south. In the same Figure, panel 2 is shown the same map for $S12 * S21 * S22$ trigger configuration, corresponding to 9.5 MeV electrons and 63 MeV protons. It is possibile to see how the intensity of the electron belts is reduced and size of the SAA is smaller as expected for higher energy protons.

VI. Conclusions

PAMELA was successfully launched on June 2006 and is currently operational in Low Earth Orbit. The satellite and the detectors are functioning correctly. It it expected that data from PAMELA will provide information on several items of cosmic rays physics, from antimatter to solar and trapped particles.

References

[Adriani 2003] O. Adriani et al., The magnetic spectrometer of the PAMELA satellite experiment, Nucl. Instr. and Meth. in Phys. Res. A 511, 72, 2003.

[Aguilar 2002] M. Aguilar et al., The Alpha Magnetic Spectrometer (AMS) on the International Space Station: Part I results from the test flight on the space shuttle, Phys. Rep. 366, 331, 2002.

[Alcaraz 2000] J. Alcaraz et al., Leptons in near earth orbit, Phys. Lett. B 484, 10, 2000.

[Asano 2006] M. Asano, S. Matsumoto, N. Okada, Y. Okada, Cosmic Positron Signature from Dark Matter in the Littlest Higgs Model with T-parity, hep-ph/0602157v1 17Feb2006.

[Asaoka 2002] Y. Asaoka et al., Measurements of Cosmic-Ray Low-Energy Antiproton and Proton Spectra in a Transient Period of Solar Field Reversal, Phys. Rev. Lett. 88, 051101, 2002; astro-ph/0109007 (2001).

[Baltz 1999] E.A. Baltz et al., Positron propagation and fluxes from neutralino annihilation in the halo, Phys. Rev. D 59, 023511, 1999.

[Barbarino 2003] G.C. Barbarino et al., The PAMELA time-of-flight system: status report, Nucl. Phys. (Proc. Suppl.) B 125, 298, 2003.

[Barwick 1998] S.W. Barwick et al., The Energy Spectra and Relative Abundances of Electrons and Positrons in the Galactic Cosmic Radiation, Astrophys. J. 498, 779, 1998.

[Barwick 1999] S. W. Barwick et al., Measurements of the Cosmic-Ray Positron Fraction From 1 to 50 GeV, Astrophys J. 482, L191, 1991; S. Coutu et al, Cosmic-Ray Positrons: Are There Primary Sources?, Astropart. Phys. 11, 429, 1999.

[Bazilevskaya 1998] G.A. Bazilevskaya and A.K. Svirzhevskaya, On The Stratospheric Measurements of Cosmic Rays, Sp. Sci. Rev. 85, 431, 1998.

[Beatty 2004] J.J. Beatty et al., New Measurement of the Cosmic-Ray Positron Fraction from 5 to 15 GeV, Phys. Rev. Lett. 93 (2004) 241102; astro-ph/0412230 (2004).

[Bergstrom 1999] L. Bergström and P. Ullio, private communication (1999).

[Bidoli 2001] V. Bidoli, A. Canestro, M. Casolino et al., In orbit performance of the space telescope NINA and Galactic cosmic-ray flux measurements, Astrophys. Journ. 132, 365, 2001.

[Bidoli 2003] V. Bidoli, M. Casolino et al., Isotope composition of secondary hydrogen and helium above the atmosphere measured by the instruments NINA and NINA-2, Journ. Geophys. Res., 108, A5, 1211, 2003.

[Boezio 1997] M. Boezio et al., The cosmic ray antiproton flux between 0.62 and 3.19 GeV measured near solar minimum activity, Astrophys. J. 487, 415, 1997.

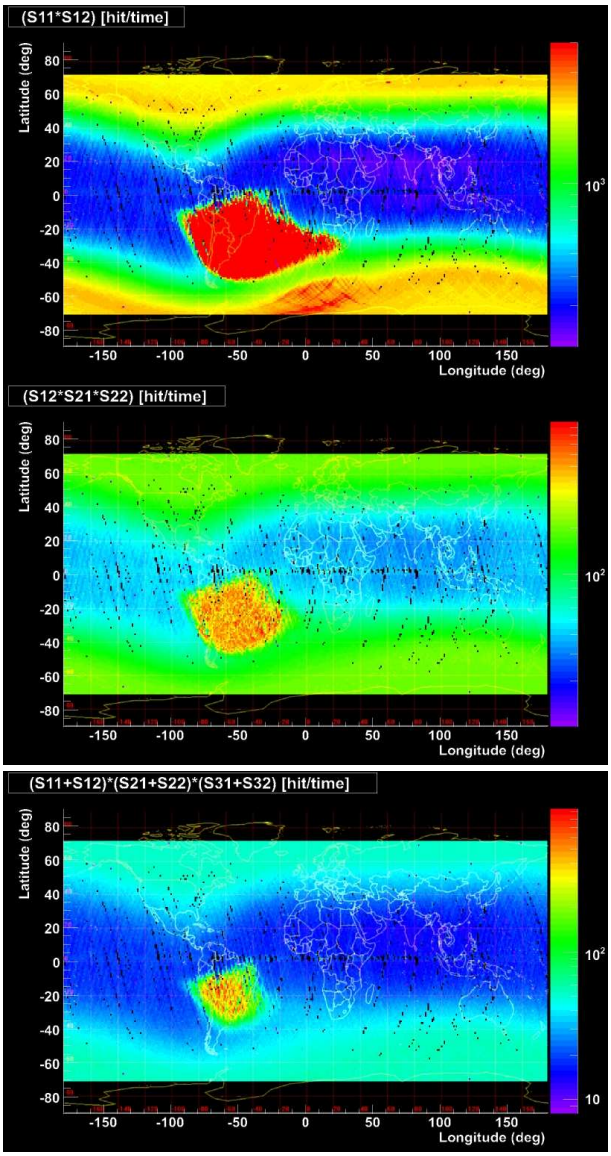

Fig. 9. Counting rates of various trigger counters of the scintillators. Top Panel: S11*S12 (p 36 MeV, e^- 2.5 MeV). Center Panel: S12*21*S22 (p 63 MeV, e^- 9.5MeV). Bottom panel: (S11*S12)*(S21+S22)*(S31+S32) (p 80 MeV, e^- 50 MeV).

[Boezio 2000] M. Boezio et al., The Cosmic-Ray Electron and Positron Spectra Measured at 1 AU during Solar Minimum Activity, Astrophys. J. 532, 653, 2000; G. Barbiellini et al., The cosmic-ray positron-to-electron ratio in the energy range 0.85 to 14 GeV, Astron. & Astrophys. 309 L15, 1996.

[Boezio 2001-a] M. Boezio et al., The Cosmic-Ray Antiproton Flux between 3 and 49 GeV, Astrophys. J. 561, 787, 2001; astro-ph/0103513 (2001).

[Boezio 2001-b] M. Boezio et al., Measurements of cosmic-ray electrons and positrons by the Wizard/CAPRICE collaboration, Advances in Space Research 27, 669, 2001.

[Boezio 2002] M. Boezio et al., "A High Granularity Imaging Calorimeter for Cosmic-Ray Physics", Nucl. Instr. and Meth. in Phys. Res. A 487, 407, 2002.

[Casolino 2001] V. Bidoli, M. Casolino et al., In-flight performance of SilEye-2 experiment and cosmic ray abundances inside the Mir space station, J. Phys. G 27, 2051, 2001.

[Casolino 2003] M. Casolino et al., Dual origins of light flashes seen in space, Nature, 422, 2003.

[Casolino 2004] M. Casolino, "Cosmic ray observation of the heliosphere with the PAMELA experiment", Advances in Space Research, **37**, 10, 1848-1852, 2006.

[Casolino 2004-a] M. Casolino, *The PAMELA Storage and Control Unit* , Adv. Sp., 37, 10, 1857, 2006.

[Casolino 2004-b] M. Casolino et al., *YODA++: A proposal for a semi-automatic space mission control*, Adv. Sp., 37, 10, 1884, 2006.

[Casolino 2005] M. Casolino et al., Detector response and calibration of the cosmic-ray detector of the Sileye-3/Alteino experiment, Adv. Space Res., 37, 9, 1691, 2006.

[Chenette 1980] D.L. Chenette, "The propagation of Jovian electrons to earth", Jour. Geophys. Res. 85, 2243, 1980.

[Chupp 1982] E. L. Chupp, D. J. Forrest, J. M. Ryan et al., Ap. J., 263 L95, 1982.

[Clem 1996] J.M. Clem et al., Solar Modulation of Cosmic Electrons, Astrophys. J. 464, 507, 1996.

[Donato 2004] F. Donato, N. Fornengo, D. Maurin, P. Salati, R. Taillet, Antiprotons in cosmic rays from neutralino annihilation, Phys. Rev. D, 69, 63501 2004.

[Eraker 1982] J.H. Eraker, Origins of the low-energy relativistic interplanetary electrons, Astrophys. Jour. 257, 862 , 1982.

[Fichtner 2001] H. Fichtner, M. S. Potgieter, S. E. S. Ferreira, B. Heber, and R. A. Burger, Effects of the solar wind termination shock on the modulation of Jovian and galactic electrons in the heliosphere, Proc. $27^{\rm th}$ Int. Cosm. Ray Conf., Hamburg, 2001, SH 3666.

[Hof 1996] M. Hof et al., Measurement of Cosmic Ray Antiprotons from 3.7 to 19 GeV, Astrophys. J. 467, L33, 1996.

[Hooper and Silk 2004] D. Hooper, J. Silk, Searching for Dark Matter with Future Cosmic Positron Experiments, Phys. Rev. D 71, 083503 2005.

[Hooper and Kribs 2004] D. Hooper, G. D. Kribs, Kaluza - Klein dark matter and the positron excess, Phys. Rev. D 70, 115004, 2004.

[Gaffey and Bilitza 1994] Gaffey, J. and D. Bilitza, NASA/National Space Science Data Center trapped radiation models, J. Spacecraft and Rockets 31, 2, 172, 1994. http://modelweb.gsfc.nasa.gov/magnetos/aeap.html

[Galper 2001] A.M. Galper et al., Measurement of primary protons and electrons in the energy range of 10^{11}–10^{13} eV in the PAMELA experiment, Proc. $27^{\rm th}$ Int. Cosm. Ray Conf., Hamburg, 2001, OG 2219.

[Golden 1987] R.L. Golden et al., Observation of cosmic ray positrons in the region from 5 to 50 GeV, Astron. & Astrophys. 188, 145, 1987.

[Golden 1994] R.L. Golden et al., Observations of cosmic-ray electrons and positrons using an imaging calorimeter, Astrophys. J. 436, 769, 1994.

[Golden 1996] R.L. Golden et al., Measurement of the Positron to Electron Ratio in the Cosmic Rays Above 5 GeV, Astrophys. J. 457, L103, 1996.

[Hisano 2006] J. Hisano, S. Matsumoto, O. Saito, M. Senami, Heavy wino-like neutralino dark matter annihilation into antiparticles, Phys. Rev. D 73, 055004, 2006.

[Kobayashi 1999] T. Kobayashi et al., Proc. 26^th Int. Cosm. Ray Conf., Salt Lake City, Vol. 3 61, 1999.

[Leske 2001] R.A. Leske et al., Observations of geomagnetic cutoff variations during solar energetic particle events and implications for the radiation environment at the Space Station, Jour. Geophys. Res. A 12, 30011, 2001.

[Lionetto 2005] A.M. Lionetto, A. Morselli, V. Zdravkovic, Uncertainties of Cosmic Ray Spectra and Detectability of Antiproton mSUGRA Contributions with PAMELA, JCAP 0509 010, 2005; astro-ph/0502406.

[Miroshnichenko 2004] L. Miroshnichenko, Solar Cosmic Rays, Kluwer, 2001.

[Mitchell 1996] J. Mitchell et al., Measurement of 0.253.2 GeV Antiprotons in the Cosmic Radiation, Phys. Rev. Lett. 76, 3057, 1996.

[Miyasaka 2003] H. Miyasaka, A. Gusev, G. Pugacheva, N.J. Schuch, U.B Jayanthi, W. Spjeldvik, Cosmic Ray Produced Antiprotons Confined in the Innermost Magnetosphere, Proc. 28^th Int. Cosm. Ray Conf., Tsukuba, Japan, 4265, 2003.

[Moskalenko 1998] I.V. Moskalenko et al., Production and Propagation of Cosmic-Ray Positrons and Electrons, Astrophys. J. 493, 694, 1998.

[Muller 1987] D. Müller et al., Cosmic-ray positrons from 10 to 20 GeV - A balloon-borne measurement using the geomagnetic east-west asymmetry, Astrophys. J. 312, 183, 1987.

[Ogliore 2001] R.C. Ogliore et al., A direct measurement of the geomagnetic cutoff for cosmic rays at space station latitudes, Proc. $27^{\rm th}$ Int. Cosm. Ray Conf., Hamburg, 2001.

[Orito 2000] S. Orito et al., Precision Measurement of Cosmic-Ray Antiproton Spectrum, Phys. Rev. Lett. 84, 1078, 2000.

[Orsi 2004] S. Orsi et al., The anticoincidence shield of the PAMELA space experiment, Advances in Space Research, **37**, 10, 1853-1856, 2006.

[Picozza 2006] P. Picozza et al., PAMELA - A Payload for Antimatter Matter Exploration and Light-nuclei Astrophysics, astro-ph/0608697, submitted to Astroparticle Physics.

[Pearce 2003] M. Pearce, The Anticounter System of the PAMELA Space Experiment, Proc. of the 28^{th} Int. Cosm. Ray Conf., Tsukuba, Japan, OG 1.5, 2125, 2003.

[Potgieter 2002] M.S. Poitgieter and S.E.S. Ferreira, Effects of the solar wind termination shock on the modulation of Jovian and galactic electrons in the heliosphere, Jour. Geophys. Res. A 7, SSH 1, 2002.

[Picozza 2006] P. Picozza et al., PAMELA - A Payload for Antimatter Matter Exploration and Light-nuclei Astrophysics, astro-ph/0608697, submitted to Astroparticle Physics.

[Profumo and Ullio 2004] S. Profumo, P. Ullio, The Role of Antimatter Searches in the Hunt for Supersymmetric Dark Matter, hep-ph/0406018v2 21Sep2004.

[Protheroe 1982] R.J. Protheroe, On the nature of the cosmic ray positron spectrum, Astrophys. J. 254, 391, 1982.

[Reames 1999] D.V. Reames, Particle acceleration at the Sun and in the heliosphere, Sp. Sci. Rev. 90, 413, 1999.

[Ryan 2000] J.M. Ryan, Long-Duration Solar Gamma-Ray Flares, Sp. Sci. Rev. 93, 581, 2000.

[Ryan 2005] J. M. Ryan, Solar Emissions, Rapp. Talk, 29th nternational Cosmic Ray Conference, Pune, 10, 357, 2005.

[Simon 1998] M. Simon et al., A New Calculation of the Interstellar Secondary Cosmic-Ray Antiprotons, Astrophys. J. 499, 250, 1998.

[Shea 2001] M.A. Shea and D.F. Smart, Solar proton and GLE event frequency: 1955-2000, Proc. $27^{\rm th}$ Int. Cosm. Ray Conf., Hamburg, 2001.

[Simpson 1974] J.A. Simpson et al., Protons and Electrons in Jupiter's Magnetic Field: Results from the University of Chicago Experiment on Pioneer 10, Science 4122, 306, 1974.

[Ullio 1999] P. Ullio, Cosmic antiprotons as a probe for neutralino dark matter?, astro-ph/9904086 (1999).